

# Highly-tunable and strong nonreciprocity in coupled nonlinear cavity magnonics

Wei Xiong\* and Zhuaxia Li

*Department of Physics, Wenzhou University, Zhejiang 325035, China*

(Dated: September 26, 2023)

Nonreciprocity, which violates Lorentz reciprocity, plays a pivotal role in quantum information processing and networks. Nevertheless, achieving a desired and highly-tunable level of nonreciprocity has proven to be a formidable challenge. Here, we propose a coupled nonlinear cavity magnonic system, consisting of two cavities, a second-order nonlinear element, and a yttrium-iron-garnet sphere for supporting Kerr magnons, to realize this sought-after highly-tunable nonreciprocity. We first derive the critical condition for switching between reciprocity and nonreciprocity with undriven magnons, then we numerically demonstrate that a strong magnonic nonreciprocity can be obtained by breaking the critical condition. When magnons are driven, we show that a strong magnonic nonreciprocity can also be attained within the critical condition. Compared to previous study, the introduced nonlinear element not only relaxes the critical condition to both the weak and strong regimes, but also offers an alternative path to adjust the magnonic nonreciprocity. Our work provides a promising avenue to realize highly-tunable nonreciprocal devices with Kerr magnons.

## I. INTRODUCTION

Thanks to the easily-engineered strong coupling between photons and magnons [1–10], which refers to the collective spin excitation in ferro- and ferrimagnetic crystals like yttrium iron garnet (YIG), a flourishing field of cavity magnonics has emerged and garnered significant attention in recent years [11–13]. Experimentally, the YIG sphere at a sub-millimeter scale and a three-dimensional microwave cavity constitute the most commonly employed cavity-magnon system [2–5]. With its flexible controllability and long coherence time for magnons, cavity magnonics has been a fertile ground for the investigation of numerous exotic phenomena [11, 14]. These include magnon memory [15], manipulation of spin currents [7, 16, 17], magnon entanglement [18–21], dissipative magnon-photon coupling [22–24], blockade [25–29], non-Hermitian physics [30–34], cooperative dynamics of polaritons [35], enhancement of spin coupling [36, 37], quantum states of magnons [38–42], microwave-to-optical transduction [43, 44], and Additionally, research efforts have extended to exploring magnon-based hybrid quantum systems, such as qubit (superconducting qubits or solid spins) magnonics [45–55], cavity magnomechanics [56–59], optomechanical cavity magnonics [60–62], and cavity optomagnonics [64–66].

With modern experimental techniques, magnon Kerr effect, arising from the magnetocrystalline anisotropy in the YIG [67], has been discovered and demonstrated [5, 68] very recently. This establishes nonlinear cavity magnonics [69] for studying novel physics including bi- and tristability [5, 70], magnon entanglement [20], magnon mediated spin-spin coupling [49, 53, 71], superradiant phase transition [72], and sensitive detection [73, 74]. Besides, magnon Kerr effect can also be used to investigate nonreciprocal devices such as non-

reciprocal entanglement [60], nonreciprocal transmission [75] and nonreciprocal higher-order sideband generation [76], which are important and essential to quantum information processing and network. However, there is a growing demand for highly-tunable nonreciprocal devices, and it still remains an open and challenging question in the field.

For this, we propose a coupled nonlinear cavity-magnon system to realize a highly-tunable magnonic nonreciprocity via adjusting various system parameters. This system comprises a cavity embedded with a second-order nonlinear element coupled to another cavity housing a YIG sphere that supports Kerr magnons (i.e., magnons with Kerr nonlinearity). We first analytically establish the critical condition for switching between reciprocity and nonreciprocity in the absence of a magnon driving field. Specifically, when the condition is unbroken, the system manifests magnonic reciprocity, but when it is broken, the system is magnonic nonreciprocal. Then we numerically demonstrate that the highly-tunable strong magnonic nonreciprocity can be achieved via tuning photon-photon coupling strength, the coefficient of the nonlinear element, or both of them. Ultimately, we prove that the external magnon driving field can induce a strong magnonic nonreciprocity with fine-tuning system parameters even when the critical condition is unbroken. Compared to the previous study [75], we show that the introduced nonlinear element not only relaxes the critical condition to both the weak and strong coupling regimes, but also provides an additional path to manipulate and achieve magnonic nonreciprocity. Our study offers a highly controllable platform for realizing nonreciprocal devices with Kerr magnons, promising versatile applications in nonlinear cavity magnonics.

The rest paper is organized as follows: In Sec. II, the model is described, and the system effective Hamiltonian is given. Then we derive the critical condition for switching between reciprocity and nonreciprocity in the absence of a magnon driving field in Sec. III. In Sec. IV, we numerically investigate magnonic nonreciprocity with vari-

---

\*xiongweiphys@wzu.edu.cn

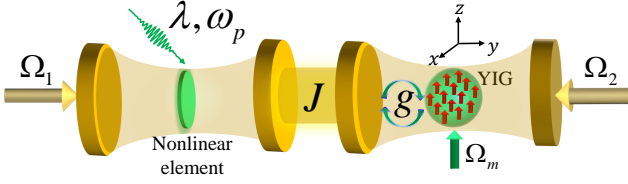


FIG. 1: Schematic diagram of the coupled nonlinear cavity magnonics. The system is composed of a PDC coupled to a MC embedded a YIG sphere with coupling strength  $J$ . The PDC can be realized by placing a second-order nonlinear element in a cavity.  $g$  is the photon-magnon coupling strength,  $\lambda$  is the parametric strength of the nonlinear element,  $\omega_p$  is the frequency of the pumping field on the nonlinear element,  $\Omega_1$ ,  $\Omega_2$ , and  $\Omega_m$  are three resonant driving fields. We here assume that the crystallographic axis of the YIG sphere is along the  $z$ -direction.

ous system parameters via breaking the critical condition given in Sec.III. Consequently, we study the magnonic nonreciprocity in the presence of the magnon driving field with the critical condition unbroken in Sec.V. Finally, a conclusion is given in Sec.VI.

## II. MODEL AND HAMILTONIAN

We consider a coupled nonlinear cavity-magnon system consisting of a parametrically driven cavity (PDC) coupled to a magnonic cavity (MC) embedded a micrometer-sized YIG sphere capable of Kerr magnons (e.g., magnons with Kerr nonlinearity), as shown in Fig. 1. The parametrically driven cavity can be realized by placing a pumping nonlinear element such as a second-order crystal in a cavity. The Kerr nonlinearity arises from the magnetocrystallographic anisotropy [34], which can be well tuned by adjusting the direction of the aligned magnetic field along the crystallographic axis [5, 68]. In addition, we here assume that three driving fields with resonant frequency  $\omega_d$  are respectively applied to two cavities and the YIG sphere. It should be noted that these external driving fields can be turned on and off at will. Taking into account the rotating-wave approximation, the Hamiltonian of the total system at the rotating frame with respect to the frequency  $\omega_d$  can be written as (setting  $\hbar = 1$ )

$$H = H_{\text{PDC}} + H_K + H_{\text{CM}} + H_{\text{PM}} + H_D, \quad (1)$$

where

$$H_{\text{PDC}} = \Delta_1 a_1^\dagger a_1 + i \frac{\lambda}{2} (a_1^\dagger a_1^\dagger - a_1 a_1) \quad (2)$$

is the Hamiltonian of the PDC, with the frequency detuning  $\Delta_1 = \omega_1 - \omega_d$  and the effective parametric strength  $\lambda$  proportional to the Rabi frequency of the pumping field. Thus, both  $\Delta_1$  and  $\lambda$  are tunable.  $\omega_1$  is the eigenfrequency of the PDC and  $a_1$  ( $a_1^\dagger$ ) is the annihilation (cre-

ation) operator of the PDC. The second term in Eq. (1),

$$H_K = \Delta_m m^\dagger m + K m^\dagger m m^\dagger m, \quad (3)$$

denotes the Hamiltonian of the Kerr magnons [20, 49] with annihilation (creation) operator  $m$  ( $m^\dagger$ ), where  $\Delta_m = \omega_m - \omega_d$ , with  $\omega_m = \gamma H$ , is the frequency detuning of the Kerr magnons from the driving field. Here,  $\gamma/2\pi = 28$  GHz/T is the gyromagnetic ratio and  $H$  is the static magnetic field. The parameter  $K = \mu_0 K_{\text{an}} \gamma / M^2 V_m$  is the Kerr coefficient, with  $\mu_0$  being the vacuum magnetic permeability,  $K_{\text{an}}$  the first-order anisotropy constant,  $M$  the saturation magnetization, and  $V_m$  the volume of the YIG sphere. Experimentally, both the value and sign of  $K$  can be tuned via varying the direction of the biased magnetic field on the YIG sphere [68]. For example, the Kerr coefficient is positive (negative) when the biased magnetic field is along the crystalline axis [100] ([110]), i.e.,  $K > 0$  ( $K < 0$ ). The Kerr magnons have been widely utilized in studying bistability [68] and tristability [70], nonreciprocity [60, 75], sensitive detection [41], quantum entanglement [20, 60] and quantum phase transition [72]. As the strength  $|K|$  is reversely proportional to the volume  $V_m$ , the strong  $K$  can be obtained by further reducing the size of the YIG sphere to nanometer scale [49]. The Hamiltonian  $H_{\text{CM}}$  in Eq. (1) characterizes the interaction between the Kerr magnons and MC, reading as

$$H_{\text{CM}} = \Delta_2 a_2^\dagger a_2 + g(a_2^\dagger m + a_2 m^\dagger), \quad (4)$$

where  $\Delta_2 = \omega_2 - \omega_d$ , with  $\omega_2$  being the eigenfrequency of the MC, is the frequency detuning of the MC from the driving field, and  $g$  is the coupling strength between the Kerr magnons and MC with the annihilation (creation) operator  $a_2$  ( $a_2^\dagger$ ). Experimentally,  $g$  in the strong coupling regime has been demonstrated with sub-millimeter-sized YIG sphere and rich physics has been observed [2–5, 8]. The fourth term

$$H_{\text{PM}} = J(a_1^\dagger a_2 + a_1 a_2^\dagger) \quad (5)$$

characterizes the interaction between the PDC and MC with the coupling strength  $J$ . The last term  $H_D$  in Eq. (1) represents the field-matter coupling Hamiltonian, given by

$$H_D = i(\Omega_1 a_1^\dagger + \Omega_2 a_2^\dagger + \Omega_m m^\dagger) + \text{H.c.}, \quad (6)$$

where  $\Omega_{1(2)} = \sqrt{\eta_{1(2)} \kappa_{1(2)}} \Omega_{1(2)}^{\text{in}}$  with  $\Omega_{1(2)}^{\text{in}} = \sqrt{P_{1(2)}/\hbar\omega_d}$  is the amplitude of the driving field applied to the PDC (MC),  $\Omega_m = \sqrt{\eta_m \gamma_m} \Omega_m^{\text{in}}$  with  $\Omega_m^{\text{in}} = \sqrt{P_m/\hbar\omega_d}$  is the amplitude of the biased magnetic field applied to the Kerr magnons in the YIG sphere. Here,  $\kappa_{1(2)}$  is the total loss rate of the PDC (MC), i.e.,  $\kappa_{1(2)} = \kappa_{1(2),0} + \kappa_{1(2),\text{ex}}$ , and  $\gamma_m$  is the total loss rate of the Kerr magnons, where  $\kappa_0$  is the intrinsic loss rate,  $\kappa_{\text{ex}}$  is the external loss,  $\eta_{1(2)}$  denotes the dimensionless external loss rate over the total loss rate of the PDC (MC), i.e.,  $\eta_{1(2)} = \kappa_{1(2),e}/\kappa_{1(2)}$ .  $\eta_m$

is the dimensionless parameter for the Kerr magnons in the YIG sphere,  $P_{1(2)}$  and  $P_m$  are the input powers of the driving fields. Note that the degenerate two-photon generation condition is taken in Eq. (1), i.e.,  $\omega_p = 2\omega_d$ .

### III. NONRECIPROCAL CONDITION

#### A. Steady-state solution

By taking dissipation into account, the dynamics of the system in Eq. (1) can be given by the quantum Langevin equation,

$$\begin{aligned}\dot{a}_1 &= -\left(i\Delta_1 + \frac{\kappa_1}{2}\right)a_1 - iJa_2 + \lambda a_1^\dagger + \Omega_1, \\ \dot{a}_2 &= -\left(i\Delta_2 + \frac{\kappa_2}{2}\right)a_2 - iJa_1 - igm + \Omega_2, \\ \dot{m} &= -\left[i(\Delta_m + 2Km^\dagger m) + \frac{\gamma_m}{2}\right]m - iga_2 + \Omega_m.\end{aligned}\quad (7)$$

In the long-time limit, the system can reach its steady state, resulting in the derivative of the expectation values ( $a_{1s}$ ,  $a_{2s}$ , and  $m_s$ ) for the system operators disappearing, i.e.,  $\dot{a}_{1s} = \dot{a}_{2s} = \dot{m}_s = 0$ . Thus, we have

$$\begin{aligned}-\left(i\Delta_1 + \frac{\kappa_1}{2}\right)a_{1s} - iJa_{2s} + \lambda a_{1s}^* + \Omega_1 &= 0, \\ -\left(i\Delta_2 + \frac{\kappa_2}{2}\right)a_{2s} - iJa_{1s} - igm_s + \Omega_2 &= 0, \\ -\left(i\tilde{\Delta}_m + \frac{\gamma_m}{2}\right)m_s - iga_{2s} + \Omega_m &= 0,\end{aligned}\quad (8)$$

where  $\tilde{\Delta}_m = \Delta_m + 2K|m_s|^2$ . From the third equation in Eq. (8),  $a_{2s}$  can be calculated directly, i.e.,

$$a_{2s} = \left[\Omega_m - (\gamma_m/2 + i\tilde{\Delta}_m)m_s\right]/ig. \quad (9)$$

Then we insert  $a_{2s}$  into the second equation in Eq. (8), and we obtain

$$\begin{aligned}a_{1s} &= [(\kappa_2/2 + i\Delta_2)\Omega_m - ig\Omega_2]/gJ \\ &\quad - \left[(\kappa_2/2 + i\Delta_2)(\gamma_m/2 + i\tilde{\Delta}_m) + g^2\right]m_s/gJ.\end{aligned}\quad (10)$$

Substituting  $a_{2s}$ ,  $a_{1s}$  and their conjugates into the first equation in Eq. (8),  $m_s$  can be given by

$$m_s = \frac{A^*\Omega + B\Omega^*}{|B|^2 - |A|^2}, \quad (11)$$

where

$$\begin{aligned}A &= \left(\frac{\kappa_1}{2} + i\Delta_1\right)\left(\frac{\kappa_2}{2} + i\Delta_2\right)\left(\frac{\gamma_m}{2} + i\tilde{\Delta}_m\right) \\ &\quad + g^2\left(\frac{\kappa_1}{2} + i\Delta_1\right) + J^2\left(\frac{\gamma_m}{2} + i\tilde{\Delta}_m\right), \\ B &= \lambda\left[\left(\frac{\kappa_2}{2} - i\Delta_2\right)\left(\frac{\gamma_m}{2} - i\tilde{\Delta}_m\right) + g^2\right], \\ \Omega &= gJ\Omega_1 + ig\left(\frac{\kappa_1}{2} + i\Delta_1 + \lambda\right)\Omega_2 \\ &\quad - \left[\left(\frac{\kappa_1}{2} + i\Delta_1\right)\left(\frac{\kappa_2}{2} + i\Delta_2\right) - \lambda\left(\frac{\kappa_2}{2} - i\Delta_2\right) + J^2\right]\Omega_m.\end{aligned}\quad (12)$$

Obviously, there is a singularity for the magnon number  $|m_s|^2 \equiv M$ , that is,  $|A| = |B|$ .

#### B. Nonreciprocal condition

By taking modulus on both sides of Eq. (11), a quintic equation related to the magnon number can be obtained, as

$$c_5M^5 + c_4M^4 + c_3M^3 + c_2M^2 + c_1M + c_0 = 0, \quad (13)$$

where  $c_i$  ( $i = 0, 1, \dots, 5$ ) are coefficients and not given here because of tedious. Note that the first three coefficients ( $c_5, c_4, c_3$ ) are independence of the Rabi frequencies of the fields  $\Omega_j$  ( $j = 1, 2, m$ ), while the rest coefficients ( $c_2, c_1, c_0$ ) are field-dependent. As a result, Eq. (13) can take distinct forms under different driving fields, showing that  $M$  may respond diversely (i.e., nonreciprocity) to the driving field applied to the PDC or MC in both the absence and presence of the magnon driving field. Specifically, when only the PDC is driven (i.e.,  $\Omega_1 \neq 0$  and  $\Omega_2 = 0$ ), Eq. (13) reduces to

$$c_5M_1^5 + c_4M_1^4 + c_3M_1^3 + c_2^{(1)}M_1^2 + c_1^{(1)}M_1 + c_0^{(1)} = 0. \quad (14)$$

But when only the MC is driven (i.e.,  $\Omega_1 = 0$  and  $\Omega_2 \neq 0$ ), Eq. (13) becomes

$$c_5M_2^5 + c_4M_2^4 + c_3M_2^3 + c_2^{(2)}M_2^2 + c_1^{(2)}M_2 + c_0^{(2)} = 0. \quad (15)$$

Explicitly, when

$$c_2^{(1)} = c_2^{(2)}, \quad c_1^{(1)} = c_1^{(2)}, \quad \text{and} \quad c_0^{(1)} = c_0^{(2)} \quad (16)$$

are simultaneously satisfied, Eqs. (14) and (15) are exactly the same, indicating that the magnon number gives the same response to the driving field of the PDC or MC, i.e.,  $M_1 = M_2$ . Otherwise,  $M_1 \neq M_2$ . Consequently, the magnon number exhibits reciprocity or nonreciprocity depending on the conditions in Eq. (16). The criteria in Eq. (16) are referred to as the critical condition for switching the reciprocity and nonreciprocity hereafter. That is, when the critical condition is broken, the magnon number behaves nonreciprocally ( $M_1 \neq M_2$ ), but when the critical condition is unbroken (satisfied), the magnon number behaves reciprocally ( $M_1 = M_2$ ). In the absence of the magnon driving field ( $\Omega_m = 0$ ), Eq. (16) can be solved analytically, giving the critical parameters as

$$J_c^{(0)} = \frac{\Omega_2}{\Omega_1} \sqrt{\Delta_1^2 + \kappa_1^2/4}, \quad \lambda_c^{(0)} = 0, \quad (17)$$

or

$$J_c = \frac{\Omega_2}{\Omega_1} \Delta_1, \quad \lambda_c = -\frac{\kappa_1}{2}. \quad (18)$$

Eq. (17) implies that the magnon number can be nonreciprocal at  $J \neq J_c^{(0)}$  without the nonlinear element ( $\lambda = \lambda_c^{(0)} = 0$ ), which has been previously investigated [75] and here we will not discuss it any more. When

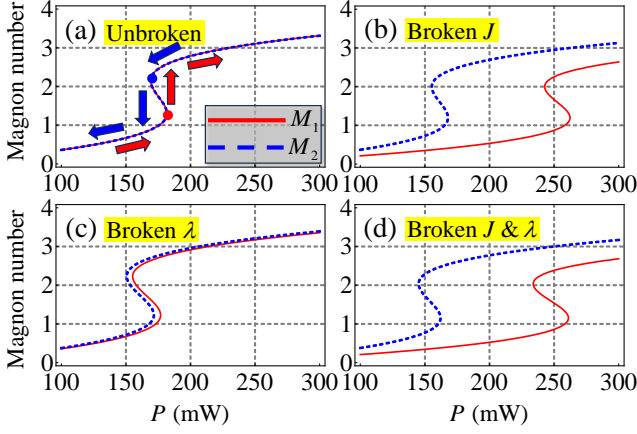


FIG. 2: The scaled magnon number as a function of the input power ( $P_1 = P_2 = P$ ) of the driving field on the PDC (MC) with the critical condition in Eq. (18) (a) unbroken and (b, c, d) broken, where (a)  $J = J_c$  and  $\lambda = \lambda_c$ , (b)  $J = 0.8J_c$  and  $\lambda = \lambda_c$ , (c)  $J = J_c$  and  $\lambda = 0.2\lambda_c$ , and (d)  $J = 0.8J_c$  and  $\lambda = 0.2\lambda_c$ . The red solid (blue dashed) curve denotes the magnon number when the PDC (MC) is driven. Other parameters are chosen as:  $\eta_1 = \eta_2 = \eta_m = 0.5$ ,  $\omega_m/2\pi = \omega_d/2\pi = 10.1$  GHz,  $g/2\pi = 41$  MHz,  $\gamma_m/2\pi = 20$  MHz,  $\kappa_1/2\pi = 5\kappa_2/2\pi = 25$  MHz,  $\Delta_1 = \Delta_2 = 4\gamma_m$ ,  $\Delta_m = \omega_m - \omega_d$ ,  $K/2\pi = 0.5$   $\mu$ Hz, and  $P_m = 0$ .

the nonlinear element ( $\lambda \neq 0$ ) is introduced, the critical parameters are modified to  $J = J_c$  and  $\lambda = \lambda_c$ , given by Eq. (18). This means that the newly included nonlinear element provides an adjustable way to produce magnonic nonreciprocity even when  $J = J_c$  is fixed. In fact, the coupling strength  $J$  between two cavities can also be tuned experimentally. Therefore, the magnonic nonreciprocity in our proposal can be accomplished by tuning both  $J$  and  $\lambda$ , resulting in more advanced controllability than the previous scheme [75]. Moreover, the induced nonlinear element can significantly *relax* the critical condition to both the weak and strong coupling regimes, because  $J_c^{(0)} \propto \sqrt{\Delta_1^2 + \kappa_1^2/4} > J_c \propto \Delta_1$ . This indicates that the reciprocal magnon number can be gained in both the strong and weak coupling regimes by including the nonlinear element, while the reciprocal magnon number can only be obtained in the strong coupling regime without the nonlinear element in the previous study [75].

#### IV. MAGNOMIC NONRECIPROCITY WITHOUT MAGNON DRIVING

Below we investigate how the magnon number behaves with various system parameters when the critical condition in Eq. (18) is unbroken or broken. In Fig. 2, we plot the scaled magnon number as a function of the input power of the driving field on the PDC or MC, where  $P_1 = P_2 = P$  is taken. Clearly, the magnon number exhibits bistability. Specifically, when the input power is swept from low to high, the magnon number increases

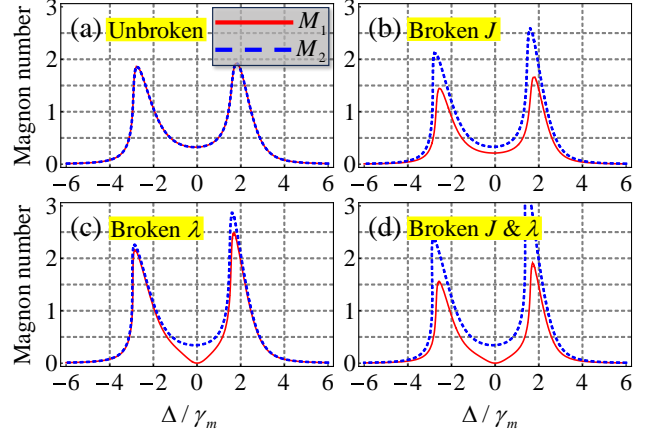


FIG. 3: The scaled magnon number as a function of the frequency detuning ( $\Delta_1 = \Delta_2 = \Delta$ ) of the PDC (MC) from the driving field with the critical condition in Eq. (18) (a) unbroken and (b,c,d) broken, where (a)  $J = J_c$  and  $\lambda = \lambda_c$ , (b)  $J = 0.8J_c$  and  $\lambda = \lambda_c$ , (c)  $J = J_c$  and  $\lambda = 0.2\lambda_c$ , and (d)  $J = 0.8J_c$  and  $\lambda = 0.2\lambda_c$ . The red solid (blue dashed) curve denotes the magnon number when the PDC (MC) is driven. Other parameters are the same as those in Fig. 2 except for  $P_1 = P_2 = P = 100$  mW,  $\Delta_m = \Delta_1 = \Delta_2 = \Delta$ , and  $\omega_d = \omega_m - \Delta$ .

along the lower stable branch to one turning point [see the red point in Fig. 2(a)] and continue to rise, and then it jumps up to the upper stable branch, as shown by the red arrow in Fig. 2(a). But when the input power is swept backwards, the magnon number declines along the higher stable branch to the other turning point [see the blue point in Fig. 2(a)], then drops to the lower stable branch [see the blue arrow in Fig. 2(a)] and continues to fall. Besides, we demonstrate numerically that the magnon number behaves reciprocally when the critical condition in Eq. (18) is unbroken. When the critical condition is broken via breaking  $J \neq J_c$  or  $\lambda \neq \lambda_c$ , however, the magnon number behaves nonreciprocally [see Figs. 2(b-d)]. Moreover, we show that the stronger nonreciprocity can be built by breaking the coupling strength  $J$  rather than the parametric strength  $\lambda$  [compared Figs. 2(b) and 2(d)] or breaking both  $J$  and  $\lambda$  simultaneously [see Fig. 2(d)].

Figure 3 shows the behavior of the scaled magnon number with the frequency detuning  $\Delta$  of the PDC or MC when the critical condition in Eq. (18) is unbroken or broken, where we set  $\Delta_1 = \Delta_2 = \Delta$  and  $P_1 = P_2 = 100$  mW. When the critical condition is unbroken, the magnon number behaves reciprocally to the driving field on the PDC or MC [see Fig. 3(a)], as predicted theoretically. By varying  $\Delta$ , the magnon number displays a two-peak profile [see Fig. 3(a)]. This is because tweaking  $\Delta$  is equal to changing the coupling strength  $J$  [see Eq. (18)]. The larger  $\Delta$ , the stronger  $J$ , resulting in two polaritons via mixing the PDC and MC. The positions of two peaks correspond to the eigenfrequencies of two polaritons. When the critical condition is broken via breaking  $J \neq J_c$  or  $\lambda \neq \lambda_c$ , the magnon number not only



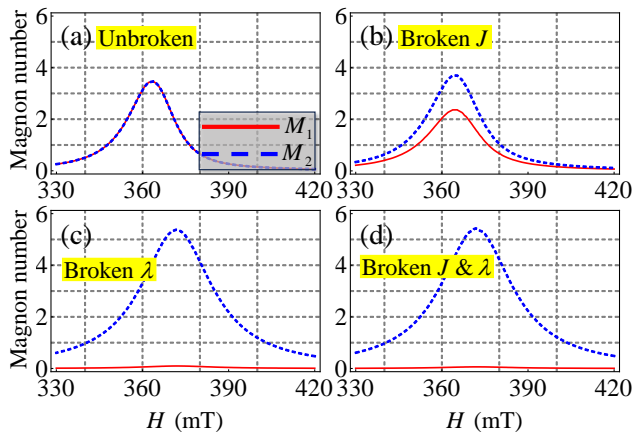


FIG. 4: The scaled magnon number as a function of the biased magnetic field ( $H = \omega_m/\gamma$ ) with the critical condition in Eq. (18) (a) unbroken and (b,c,d) broken, where (a)  $J = J_c$  and  $\lambda = \lambda_c$ , (b)  $J = 0.8J_c$  and  $\lambda = \lambda_c$ , (c)  $J = J_c$  and  $\lambda = 0.2\lambda_c$ , and (d)  $J = 0.8J_c$  and  $\lambda = 0.2\lambda_c$ . The red solid (blue dashed) curve denotes the magnon number when the PDC (MC) is driven. Other parameters are the same as those in Fig. 2 except for  $P_1 = P_2 = P = 100$  mW and  $\Delta_1 = \Delta_2 = \Delta = 0.1\gamma_m$ .

has a two-peak profile, but also behaves nonreciprocally [see Figs. 3(b-d)]. When only the coupling strength  $J$  is broken ( $J \neq J_c$  while  $\lambda = \lambda_c$ ), the parameter space of  $\Delta$  for observing the magnonic nonreciprocity is broader than the case of breaking the parametric strength only ( $\lambda = \lambda_c$  while  $J = J_c$ ), via comparing Figs. 3(b) and 3(c). Furthermore, the nonreciprocity caused by breaking  $J$  is significantly stronger at two peaks than that induced by breaking  $\lambda$ , but as one approaches the near resonance ( $\Delta \approx 0$ ), the situation reverses. Actually, the cooperative effect of breaking  $J$  and  $\lambda$  both yields the better nonreciprocity and broader parameter range [see Fig. 3(d)].

We then study the behavior of the magnon number with the biased magnetic field  $H$  when the critical condition in Eq. (18) is unbroken or broken, as shown in Fig. 4. When the critical condition is unbroken, the magnon number is reciprocal and exhibits a Lorentz profile with  $H$  for the driving field on the PDC or MC [see Fig. 4(a)]. But when the crucial condition is broken, the magnon number gets the nonreciprocal behavior [see Figs. 4(b-d)]. Figure 4(b) further shows that the magnon number caused by the driving field on the PDC is slightly suppressed around  $H = 370$  mT (see the blue dashed curve) by breaking  $J$ , whereas the magnon number caused by the driving field on the MC is enhanced a little (see the red solid curve), leading to visible nonreciprocity. From Fig. 4(c), one can see that a much stronger nonreciprocity can be obtained by breaking the critical condition  $\lambda = \lambda_c$ , via greatly enhancing (fully suppressed) the magnon number caused by the driving field on the PDC (MC). When both  $J = J_c$  and  $\lambda = \lambda_c$  are broken, the produced nonreciprocity is completely dominant by breaking

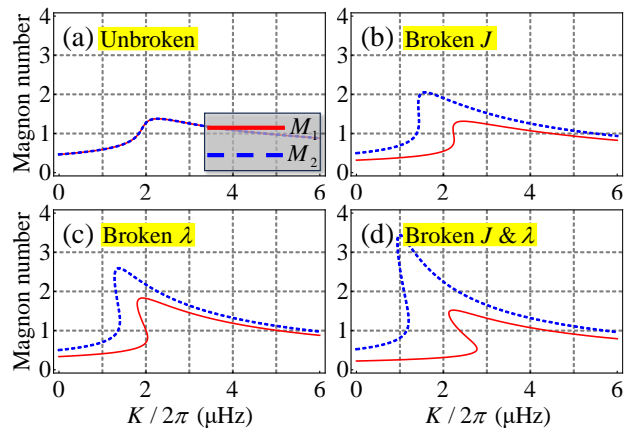


FIG. 5: The scaled magnon number as a function of the Kerr coefficient ( $K$ ) with the critical condition in Eq. (18) (a) unbroken and (b,c,d) broken, where (a)  $J = J_c$  and  $\lambda = \lambda_c$ , (b)  $J = 0.8J_c$  and  $\lambda = \lambda_c$ , (c)  $J = J_c$  and  $\lambda = 0.2\lambda_c$ , and (d)  $J = 0.8J_c$  and  $\lambda = 0.2\lambda_c$ . The red solid (blue dashed) curve denotes the magnon number when the PDC (MC) is driven. Other parameters are the same as those in Fig. 2 except for  $P_1 = P_2 = P = 100$  mW and  $\Delta_1 = \Delta_2 = \Delta = \gamma_m$ .

$\lambda = \lambda_c$  [see Fig. 4(d)], and the nonreciprocity induced by breaking  $J = J_c$  can thus be ignored.

Finally, we numerically check the impact of the Kerr coefficient on the scaled magnon number when the critical condition in Eq. (18) is unbroken or broken, as illustrated in Fig. 5. We show that the magnon number reciprocally responds to the driving field on the PDC or MC with  $K$  when the critical condition is unbroken, resulting in a  $S$ -like pattern in the profile [see Fig. 5(a)]. But when the critical condition is broken via breaking  $J = J_c$  [see Fig. 5(a)], the magnon number responds nonreciprocally to the driving field on the PDC or MC [see Fig. 5(b)]. In particular, the magnon number is boosted (suppressed) and gets a redshift (blueshift) for  $\Omega_1 \neq 0$  ( $\Omega_2 \neq 0$ ), giving rise to a sub- $S$  pattern in the profile. But if we break the critical condition by breaking  $\lambda = \lambda_c$  such as  $\lambda = 0.2\lambda_c$ , the magnon numbers at the cases of  $\Omega_1 = 0$  or  $\Omega_2 = 0$  are nonreciprocally enhanced and red shifted, and thus the profile becomes a genuine  $S$  pattern [see Fig. 5(c)]. By combining the cooperative effect of breaking both  $J = J_c$  and  $\lambda = \lambda_c$ , the magnon number responds to the driving field on the PDC is significantly improved and has a big redshift, while the magnon number responds to the driving field on the MC gains a bit enhancement and blueshift, as given by Fig. 5(d). Besides, the cooperative effect can give rise to a standard  $S$  pattern, i.e., bistability, in the profile for the case of  $\Omega_2 \neq 0$  [see the red curve in Fig. 5(d)].

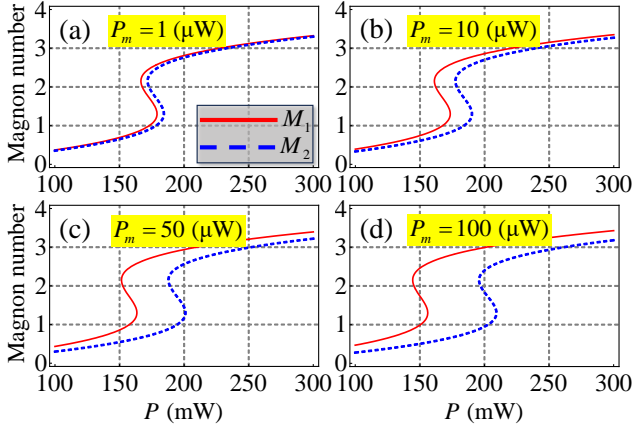


FIG. 6: The scaled magnon number as a function of the input power ( $P_1 = P_2 = P$ ) of the driving field on the PDC (MC) with the magnon driving field and the critical condition in Eq. (18) unbroken. In (a)  $P_m = 1 \mu\text{W}$ , (b)  $P_m = 10 \mu\text{W}$ , (c)  $P_m = 50 \mu\text{W}$ , and (d)  $P_m = 100 \mu\text{W}$ . The red solid (blue dashed) curve denotes the magnon number when the PDC (MC) is driven. Other parameters the same as those in Fig. 2.

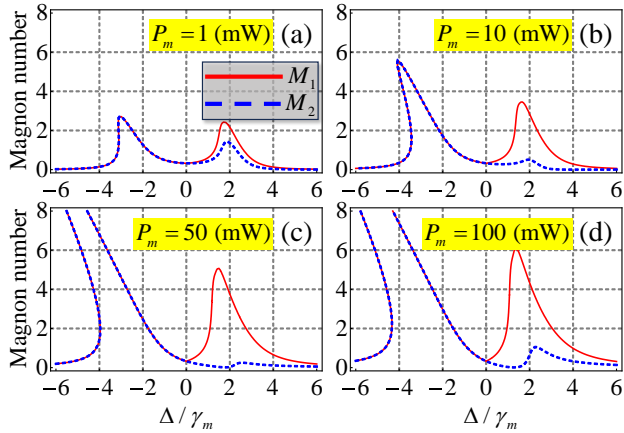


FIG. 7: The scaled magnon number as a function of the frequency detuning ( $\Delta_1 = \Delta_2 = \Delta$ ) of the PDC (MC) from the driving field in the presence of the magnon driving field with the critical condition in Eq. (18) unbroken. In (a)  $P_m = 1 \text{ mW}$ , (b)  $P_m = 10 \text{ mW}$ , (c)  $P_m = 50 \text{ mW}$ , and (d)  $P_m = 100 \text{ mW}$ . The red solid (blue dashed) curve denotes the magnon number when the PDC (MC) is driven. Other parameters the same as those in Fig. 3.

## V. MAGNONIC NONRECIPROCALITY WITH MAGNON DRIVING

It should be noted that the critical condition in Eq. (18) is given in the case of  $\Omega_m = 0$ , i.e., the magnons in the YIG sphere are not driven. When the magnon driving field is taken into account,  $\Omega_m \neq 0$ , the condition in Eq. (18) is naturally broken and adjusted. This means that the magnonic nonreciprocity can be predicted by imposing an additional driving field to the magnons.

To elucidate the impact of the magnon driving field on

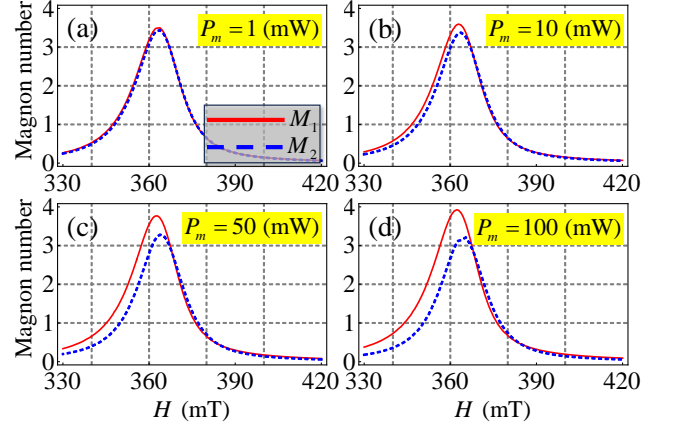


FIG. 8: The scaled magnon number as a function of the biased magnetic field ( $H = \omega_m/\gamma$ ) in the presence of the magnon driving field with the critical condition in Eq. (18) unbroken. In (a)  $P_m = 1 \text{ mW}$ , (b)  $P_m = 10 \text{ mW}$ , (c)  $P_m = 50 \text{ mW}$ , and (d)  $P_m = 100 \text{ mW}$ . The red solid (blue dashed) curve denotes the magnon number when the PDC (MC) is driven. Other parameters the same as those in Fig. 4.

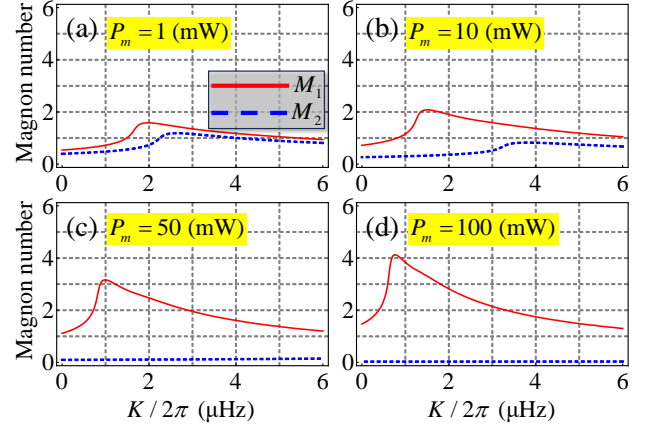


FIG. 9: The scaled magnon number as a function of the Kerr coefficient ( $K$ ) in the presence of the magnon driving field with the critical condition in Eq. (18) unbroken. In (a)  $P_m = 1 \text{ mW}$ , (b)  $P_m = 10 \text{ mW}$ , (c)  $P_m = 50 \text{ mW}$ , and (d)  $P_m = 100 \text{ mW}$ . The red solid (blue dashed) curve denotes the magnon number when the PDC (MC) is driven. Other parameters the same as those in Fig. 5.

the magnon number, we illustrate the relationship between the magnon number and various parameters with different  $P_m$  in Figs. (6)-(9). Figure 6 shows that the magnon number displays nonreciprocal bistability in the presence of the magnon driving field. For the weak power ( $P_m = 1$ ), a dim nonreciprocal bistability for the magnon number can be predicted [see Fig. 6(a)]. With increasing the power of the magnon driving field, the nonreciprocity becomes more pronounced and stronger [see Fig. 6(b)-6(d)]. Further, we find that the range of the input power for observing the nonreciprocity is broaden. By investigating the magnon number with the frequency detuning

in Fig. 7, it can be seen that the magnon number behaves nonreciprocally in the red-detuned regime ( $\Delta > 0$ ) in the presence of the magnon driving field ( $P_m \neq 0$ ), while it behaves reciprocally in the blue-detuned regime ( $\Delta < 0$ ). Figure 7 also reveals that the stronger power of the magnon driving field can give rise to a stronger nonreciprocity, via boosting (suppressing) the magnon number caused by the driving field on the MC (PDC). In Fig. 8, we plot the magnon number as a function of the magnetic field  $H$  with different powers of the magnon driving field. Obviously, the visible nonreciprocity can only be observed in the region of  $H < 365$  mT, assisted by a strong power of the magnon driving field such as  $P_m = 50$  mW [see Fig. 8(c)] or  $P_m = 100$  mW [see Fig. 8(d)]. In the opposite region, the magnon number behaves reciprocally. We further depict the magnon number with the Kerr coefficient in the presence of the magnon driving field in Fig. 9. Clearly, the magnon number responding to the driving field on the PMC (MC) increases (reduces) and has a significant redshift (blueshift) with increasing  $P_m$ . This indicates that a strong nonreciprocity can be produced by using the powerful magnon driving field.

## VI. CONCLUSION

In summary, we have proposed a coupled nonlinear cavity-magnon system, consisting of a cavity embedded

a nonlinear element coupled to another cavity including Kerr magnons in a YIG sphere, to realize magnonic nonreciprocity. We first analytically derive the critical condition for predicting the magnonic nonreciprocity in the absence of the magnon driving field. Then, we numerically demonstrate that the strong magnonic nonreciprocity can be obtained in the case of breaking the critical condition, via tuning the two-cavity coupling strength  $J$ , the parametric coupling strength  $\lambda$ , or both of them. We further investigate the magnonic nonreciprocity in the presence of the magnon driving field when the critical condition is kept. The result shows that the strong power of the magnon driving field can give rise to strong nonreciprocity, which can be observed in a certain parameter space. Compared to the prior study without the nonlinear element [75], we find that the introduced nonlinear element not only can loosen the criterion in both the weak and strong coupling regimes, making the proposal more feasible, but also provides an additional path to manipulate the magnonic nonreciprocity. Our study paves a potential platform to realize highly-tunable nonreciprocal devices with Kerr magnons.

This paper is supported by the National Natural Science Foundation of China (Grant No. 11804074).

- 
- [1] H. Huebl, C. W. Zollitsch, J. Lotze, F. Hocke, M. Greifenstein, A. Marx, R. Gross, and S. T. B. Goennenwein, High Cooperativity in Coupled Microwave Resonator Ferrimagnetic Insulator Hybrids, *Phys. Rev. Lett.* **111**, 127003 (2013).
  - [2] Y. Tabuchi, S. Ishino, T. Ishikawa, R. Yamazaki, K. Usami, and Y. Nakamura, Hybridizing Ferromagnetic Magnons and Microwave Photons in the Quantum Limit, *Phys. Rev. Lett.* **113**, 083603 (2014).
  - [3] X. Zhang, C.-L. Zou, L. Jiang, and H. X. Tang, Strongly Coupled Magnons and Cavity Microwave Photons, *Phys. Rev. Lett.* **113**, 156401 (2014).
  - [4] M. Goryachev, W. G. Farr, D. L. Creedon, Y. Fan, M. Kostylev, and M. E. Tobar, High-Cooperativity Cavity QED with Magnons at Microwave Frequencies, *Phys. Rev. Applied* **2**, 054002 (2014).
  - [5] Y. P. Wang, G. Q. Zhang, D. Zhang, X. Q. Luo, W. Xiong, S. P. Wang, T. F. Li, C. M. Hu, and J. Q. You, Magnon Kerr effect in a strongly coupled cavity-magnon system, *Phys. Rev. B* **94**, 224410 (2016).
  - [6] B. Bhoi, T. Cliff, I. S. Maksymov, M. Kostylev, R. Aiyar, N. Venkataramani, S. Prasad, and R. L. Stamps, Study of photon-magnon coupling in a YIG-film split-ring resonant system, *J. Appl. Phys.* **116**, 243906 (2014).
  - [7] L. Bai, M. Harder, Y. P. Chen, X. Fan, J. Q. Xiao, and C.-M. Hu, Spin Pumping in Electrodynamically Coupled Magnon-Photon Systems, *Phys. Rev. Lett.* **114**, 227201 (2015).
  - [8] D. Zhang, X. M. Wang, T. F. Li, X. Q. Luo, W. Wu, F. Nori, and J. Q. You, Cavity quantum electrodynamics with ferromagnetic magnons in a small yttrium-iron-garnet sphere, *npj Quantum Inf.* **1**, 15014 (2015).
  - [9] Y. Li, T. Polakovic, Y.-L. Wang, J. Xu, S. Lendinez, Z. Zhang, J. Ding, T. Khaire, H. Saglam, R. Divan, J. Pearson, W.-K. Kwok, Z. Xiao, V. Novosad, A. Hoffmann, and W. Zhang, Strong Coupling between Magnons and Microwave Photons in On-Chip Ferromagnet-Superconductor Thin-Film Devices, *Phys. Rev. Lett.* **123**, 107701 (2019).
  - [10] J. T. Hou and L. Liu, Strong Coupling between Microwave Photons and Nanomagnet Magnons, *Phys. Rev. Lett.* **123**, 107702 (2019).
  - [11] B. Z. Rameshti, S. V. Kusminskiy, J. A. Haigh, K. Usami, D. Lachance-Quirion, Y. Nakamura, C. M. Hu, H. X. Tang, G. E. W. Bauer, and Y. M. Blanter, Cavity magnonics, *Phys. Rep.* **979**, 1 (2022).
  - [12] D. Lachance-Quirion, Y. Tabuchi, A. Gloppe, K. Usami, and Y. Nakamura, Hybrid quantum systems based on magnonics, *Appl. Phys. Express* **12**, 070101 (2019).
  - [13] H. Y. Yuan, Y. Cao, A. Kamra, R. A. Duine, and P. Yan, Quantum magnonics: When magnon spintronics meets quantum information science, *Phys. Rep.* **965**, 1 (2022).
  - [14] Y. P. Wang and C.-M. Hu, Dissipative couplings in cavity magnonics, *J. Appl. Phys.* **127**, 130901 (2020).
  - [15] X. Zhang, C.-L. Zou, N. Zhu, F. Marquardt, L. Jiang, and H. X. Tang, Magnon dark modes and gradient memory, *Nat. Commun.* **6**, 8914 (2015).
  - [16] L. Bai, M. Harder, P. Hyde, Z. Zhang, C. M. Hu, Y. P.

- Chen, and J. Q. Xiao, Cavity Mediated Manipulation of Distant Spin Currents Using a Cavity-Magnon-Polariton, *Phys. Rev. Lett.* **118**, 217201 (2017).
- [17] D. Mukhopadhyay, J. M. P. Nair, and G. S. Agarwal, Quantum amplification of spin currents in cavity magnonics by a parametric drive induced long-lived mode, *Phys. Rev. B* **106**, 184426 (2022).
- [18] H. Y. Yuan, S. Zheng, Z. Ficek, Q. Y. He, and M.-H. Yung, Enhancement of magnon-magnon entanglement inside a cavity, *Phys. Rev. B* **101**, 014419 (2020).
- [19] V. A. Mousolou, Y. Liu, A. Bergman, A. Delin, O. Eriksson, M. Pereiro, D. Thonig, and E. Sjöqvist, Phys. Magnon-magnon entanglement and its quantification via a microwave cavity, *Phys. Rev. B* **104**, 224302 (2021).
- [20] Z. Zhang, Marlan O. Scully, and Girish S. Agarwal, Quantum entanglement between two magnon modes via Kerr nonlinearity driven far from equilibrium, *Phys. Rev. Research* **1**, 023021 (2019).
- [21] Y. Ren, J. Xie, X. Li, S. Ma, and F. Li, Long-range generation of a magnon-magnon entangled state, *Phys. Rev. B* **105**, 094422 (2022).
- [22] M. Harder, Y. Yang, B. M. Yao, C. H. Yu, J. W. Rao, Y. S. Gui, R. L. Stamps, and C. M. Hu, Level Attraction Due to Dissipative Magnon-Photon Coupling, *Phys. Rev. Lett.* **121**, 137203 (2018).
- [23] V. L. Grigoryan, K. Shen, and K. Xia, Synchronized spin-photon coupling in a microwave cavity, *Phys. Rev. B* **98**, 024406 (2018).
- [24] Y. P. Wang, J. W. Rao, Y. Yang, P. C. Xu, Y. S. Gui, B. M. Yao, J. Q. You, and C.-M. Hu, Nonreciprocity and Unidirectional Invisibility in Cavity Magnonics, *Phys. Rev. Lett.* **123**, 127202 (2019).
- [25] R. Huang, A. Miranowicz, J. Q. Liao, F. Nori, and H. Jing, Nonreciprocal Photon Blockade, *Phys. Rev. Lett.* **121**, 153601 (2018).
- [26] X. Y. Yao, H. Ali, and P. B. Li, Nonreciprocal Phonon Blockade in a Spinning Acoustic Ring Cavity Coupled to a Two-Level System, *Phys. Rev. Applied* **17**, 054004 (2022).
- [27] Y. Wang, W. Xiong, Z. Xu, G. Q. Zhang, and J. Q. You, Dissipation-induced nonreciprocal magnon blockade in a magnon-based hybrid system, *Sci. China Phys. Mech. Astron.* **65**, 260314 (2022).
- [28] J. K. Xie, S. L. Ma, and F. L. Li, Quantum-interference enhanced magnon blockade in an yttrium-iron-garnet sphere coupled to superconducting circuits, *Phys. Rev. A* **101**, 042331 (2020).
- [29] F. Wang, C. Gou, J. Xu, and C. Gong, Hybrid magnon-atom entanglement and magnon blockade via quantum interference, *Phys. Rev. A* **106**, 013705 (2022).
- [30] D. Zhang, X. Q. Luo, Y. P. Wang, T. F. Li, and J. Q. You, Observation of the exceptional point in cavity magnon-polaritons, *Nat. Commun.* **8**, 1368 (2017).
- [31] M. Harder, L. Bai, P. Hyde, and C. M. Hu, Topological properties of a coupled spin-photon system induced by damping, *Phys. Rev. B* **95**, 214411 (2017).
- [32] Y. Cao and P. Yan, Exceptional magnetic sensitivity of PT-symmetric cavity magnon polaritons, *Phys. Rev. B* **99**, 214415 (2019).
- [33] J. Zhao, Y. Liu, L. Wu, C. K. Duan, Y. Liu, and J. Du, Observation of Anti-PT-Symmetry Phase Transition in the Magnon-Cavity-Magnon Coupled System, *Phys. Rev. Appl.* **13**, 014053 (2020).
- [34] G.-Q. Zhang and J. Q. You, Higher-order exceptional point in a cavity magnonics system, *Phys. Rev. B* **99**, 054404 (2019).
- [35] B. Yao, Y. S. Gui, J. W. Rao, S. Kaur, X. S. Chen, W. Lu, Y. Xiao, H. Guo, K. P. Marzlin, and C. M. Hu, Cooperative polariton dynamics in feedback-coupled cavities, *Nat. Commun.* **8**, 1437 (2017).
- [36] M. Tian, M. Wang, G.-Q. Zhang, H.-C. Li, and W. Xiong, Critical cavity-magnon polariton mediated strong long-distance spin-spin coupling, arXiv:2304.13553.
- [37] X. L. Hei, X. L. Dong, J. Q. Chen, C. P. Shen, Y. F. Qiao, and P. B. Li, Enhancing spin-photon coupling with a micromagnet, *Phys. Rev. A* **103**, 043706 (2021).
- [38] D. Xu, X.-K. Gu, H.-K. Li, Y.-C. Weng, Y.-P. Wang, J. Li, H. Wang, S.-Y. Zhu, and J. Q. You, Quantum Control of a Single Magnon in a Macroscopic Spin System, *Phys. Rev. Lett.* **130**, 193603 (2023).
- [39] H. Y. Yuan, P. Yan, S. Zheng, Q. Y. He, K. Xia, and M.-H. Yung, Steady Bell State Generation via Magnon-Photon Coupling, *Phys. Rev. Lett.* **124**, 053602 (2020).
- [40] F. X. Sun, S. S. Zheng, Y. Xiao, Q. Gong, Q. He, and K. Xia, Remote Generation of Magnon Schrödinger Cat State via Magnon-Photon Entanglement, *Phys. Rev. Lett.* **127**, 087203 (2021).
- [41] G. Q. Zhang, W. Feng, W. Xiong, Q. P. Su, and C. P. Yang, Generation of long-lived W states via reservoir engineering in dissipatively coupled systems, *Phys. Rev. A* **107**, 012410 (2023).
- [42] S. F. Qi and J. Jing, Generation of Bell and Greenberger-Horne-Zeilinger states from a hybrid qubit-photon-magnon system, *Phys. Rev. A* **105**, 022624 (2022).
- [43] R. Hisatomi, A. Osada, Y. Tabuchi, T. Ishikawa, A. Noguchi, R. Yamazaki, K. Usami, and Y. Nakamura, Bidirectional conversion between microwave and light via ferromagnetic magnons, *Phys. Rev. B* **93**, 174427 (2016).
- [44] N. Zhu, X. Zhang, X. Han, C. L. Zou, C. Zhong, C. H. Wang, L. Jiang, and H. X. Tang, Waveguide cavity optomagnonics for broadband multimode microwave-to-optics conversion, *Optica* **7**, 1291 (2020).
- [45] Y. Tabuchi, S. Ishino, A. Noguchi, T. Ishikawa, R. Yamazaki, K. Usami, and Y. Nakamura, Coherent coupling between a ferromagnetic magnon and a superconducting qubit, *Science* **349**, 405 (2015).
- [46] D. Lachance-Quirion, S. P. Wolski, Y. Tabuchi, S. Kono, K. Usami, and Y. Nakamura, Entanglement-based single-shot detection of a single magnon with a superconducting qubit, *Science*, **367**, 425 (2020).
- [47] O. V. Dobrovolskiy, R. Sachser, T. Brächer, T. Böttcher, V. V. Kruglyak, R. V. Vovk, V. A. Shklovskij, M. Huth, B. Hillebrands, and A. V. Chumak, Magnon-fluxon interaction in a ferromagnet/superconductor heterostructure, *Nat. Phys.* **15**, 477 (2019).
- [48] S. P. Wolski, D. Lachance-Quirion, Y. Tabuchi, S. Kono, A. Noguchi, K. Usami, and Y. Nakamura, Dissipation-Based Quantum Sensing of Magnons with a Superconducting Qubit, *Phys. Rev. Lett.* **125**, 117701 (2020).
- [49] W. Xiong, M. Tian, G.-Q. Zhang, and J. Q. You, Strong long-range spin-spin coupling via a Kerr magnon interface, *Physical Review B* **105**, 245310 (2022).
- [50] T. Neuman, D. S. Wang, and P. Narang, Nanomagnonic Cavities for Strong Spin-Magnon Coupling and Magnon-Mediated Spin-Spin Interactions, *Phys. Rev. Lett.* **125**, 247702 (2020).
- [51] D. S. Wang, T. Neuman, and P. Narang, Spin Emitters beyond the Point Dipole Approximation in Nano-



- magnonic Cavities, *J. Phys. Chem. C* **125**, 6222 (2021).
- [52] D. S. Wang, M. Haas, and P. Narang, Quantum Interfaces to the Nanoscale, *ACS Nano* **15**, 7879 (2021).
- [53] I. C. Skogvoll, J. Lidal, J. Danon, and A. Kamra, Tunable anisotropic quantum Rabi model via magnon spin-qubit ensemble, *Phys. Rev. Applied* **16**, 064008 (2021).
- [54] L. Trifunovic, F. L. Pedrocchi, and D. Loss, Long-Distance Entanglement of Spin Qubits via Ferromagnet, *Phys. Rev. X* **3**, 041023 (2013).
- [55] M. Fukami, D. R. Candido, D. D. Awschalom, and M. E. Flatté, Opportunities for Long-Range Magnon-Mediated Entanglement of Spin Qubits via On- and Off-Resonant Coupling, *PRX Quantum* **2**, 040314 (2021).
- [56] X. Zhang, C. L. Zou, L. Jiang, and H. X. Tang, Cavity magnomechanics, *Sci. Adv.* **2**, e1501286 (2016).
- [57] J. Li, S.-Y. Zhu, and G. S. Agarwal, Magnon-Photon-Phonon Entanglement in Cavity Magnomechanics, *Phys. Rev. Lett.* **121**, 203601 (2018).
- [58] R.-C. Shen, J. Li, Z.-Y. Fan, Y.-P. Wang, and J. Q. You, Mechanical Bistability in Kerr-modified Cavity Magnomechanics, *Phys. Rev. Lett.* **129**, 123601 (2022).
- [59] J. Li, Y.-P. Wang, W.-J. Wu, S.-Y. Zhu, and J. Q. You, Quantum Network with Magnonic and Mechanical Nodes, *PRX Quantum* **2**, 040344 (2021).
- [60] J. Chen, X.-G. Fan, W. Xiong, D. Wang, and L. Ye, Nonreciprocal entanglement in cavity-magnon optomechanics, *Phys. Rev. B* **108**, 024105 (2023).
- [61] I. Proskurin, A. S. Ovchinnikov, J. Kishine, and R. L. Stamps, Cavity optomechanics of topological spin textures in magnetic insulators, *Phys. Rev. B* **98**, 220411(R) (2018).
- [62] W. Xiong, M. Wang, G.-Q. Zhang, and J. Chen, Optomechanical-interface-induced strong spin-magnon coupling, *Phys. Rev. A* **107**, 033516 (2023).
- [63] Y.-P. Gao, C. Cao, T.-J. Wang, Y. Zhang, and C. Wang, Cavity-mediated coupling of phonons and magnons, *Phys. Rev. A* **96**, 023826 (2017).
- [64] X. Zhang, N. Zhu, C.-L. Zou, and H. X. Tang, Optomagnonic Whispering Gallery Microresonators, *Phys. Rev. Lett.* **117**, 123605 (2016).
- [65] A. Osada, R. Hisatomi, A. Noguchi, Y. Tabuchi, R. Yamazaki, K. Usami, M. Sadgrove, R. Yalla, M. Nomura, and Y. Nakamura, Cavity Optomagnonics with Spin-Orbit Coupled Photons, *Phys. Rev. Lett.* **116**, 223601 (2016).
- [66] J. A. Haigh, A. Nunnenkamp, A. J. Ramsay, and A. J. Ferguson, Triple-Resonant Brillouin Light Scattering in Magneto-Optical Cavities, *Phys. Rev. Lett.* **117**, 133602 (2016).
- [67] G. Q. Zhang, Y. P. Wang, and J. Q. You, Theory of the magnon Kerr effect in cavity magnonics, *Sci. China: Phys. Mech. Astron.* **62**, 987511 (2019).
- [68] Y. P. Wang, G. Q. Zhang, D. Zhang, T. F. Li, C. M. Hu, and J. Q. You, Bistability of Cavity Magnon Polaritons, *Phys. Rev. Lett.* **120**, 057202 (2018).
- [69] S. Zheng, Z. Wang, Y. Wang, F. Sun, Q. He, P. Yan, and H. Y. Yuan, Tutorial: Nonlinear magnonics, arXiv:2303.16313.
- [70] R. C. Shen, Y. P. Wang, J. Li, S. Y. Zhu, G. S. Agarwal, and J. Q. You, Long-Time Memory and Ternary Logic Gate Using a Multistable Cavity Magnonic System, *Phys. Rev. Lett.* **127**, 183202 (2021).
- [71] F.-Z. Ji and J.-H. An, Kerr-Nonlinearity-Induced Strong Spin-Magnon Coupling, arXiv:2308.05927.
- [72] G. Liu, W. Xiong, and Z. J. Ying, Switchable superradiant phase transition with Kerr magnons, *Phys. Rev. A* **108**, 033704 (2023).
- [73] G.-Q. Zhang, Y. Wang, and W. Xiong, Detection sensitivity enhancement of magnon Kerr nonlinearity in cavity magnonics induced by coherent perfect absorption, *Phys. Rev. B* **107**, 064417 (2023).
- [74] J. M. P. Nair, D. Mukhopadhyay, and G. S. Agarwal, Enhanced sensing of weak anharmonicities through coherences in dissipatively coupled anti-PT symmetric systems, *Phys. Rev. Lett.* **126**, 180401 (2021).
- [75] C. Kong, H. Xiong, and Y. Wu, Magnon-Induced Nonreciprocity Based on the Magnon Kerr Effect, *Phys. Rev. Applied* **12**, 034001 (2019).
- [76] M. Wang, C. Kong, Z.-Y. Sun, D. Zhang, Y.-Y. Wu, and L.-L. Zheng, Nonreciprocal high-order sidebands induced by magnon Kerr nonlinearity, *Phys. Rev. A* **104**, 033708 (2021).